Title

Understanding shallow gas occurrences in the Gulf of Lions

Journal

Geo-Marine Letters, 27

ISSN

0276-0460

Authors

Garcia-Garcia, A.
Tesi, T.
Orange, D.
et al.

Publication Date

2007-06-01

DOI

10.1007/s00367-007-0067-1

Peer reviewed

Understanding shallow gas occurrences in the Gulf of Lions

García-García[1,2], A., Tesi[3], T., Orange[2,1], D., Lorenson[4], T., Miserocchi[3], S., Langone[3], L., Herbert[2], I., Dougherty[4], J.

[1]Department of Earth Sciences, UCSC, Santa Cruz, CA 95064, USA
[2]AOA Geophysics Inc., Moss Landing, CA 95039, USA
[3]CNR-ISMAR, 40129 Bologna, Italy
[4]USGS, Menlo Park, CA 94025, USA

ABSTRACT

New coring data have been acquired along the western Gulf of Lions showing anomalous concentrations of methane (up to 95720 ppm) off the Rhône prodelta and the head of the southern canyons Lacaze-Duthiers and Cap de Creus. Sediment cores were acquired with box and kasten cores during 2004-2005 on several EuroSTRATAFORM cruises. Anomalous methane concentrations are discussed and integrated with organic carbon data. Sampled sites include locations where previous surveys identified acoustic anomalies in high-resolution seismic profiles, which may be related to the presence of gas. Interpretation of the collected data has enabled us to discuss the nature of shallow gas along the Gulf of Lions and its association with recent sedimentary dynamics.

The Rhône prodelta flood deposits deliver significant amounts of terrigenous organic matter that can be rapidly buried, effectively removing this organic matter from aerobic oxidation and biological uptake, and leading to the potential for methanogenesis with burial. Away from the flood-related sediments off the Rhône delta, the organic matter is being reworked and remineralized on its way along the western coast of the Gulf of Lions, with the result that the recent deposits in the canyon contain little reactive carbon.

In the southernmost canyons, Lacaze-Duthiers and Cap de Creus, the gas analyses show relatively little shallow gas in the core samples. Samples with anomalous gas (up to 4982 ppm of methane) are limited to local areas where the samples also show higher amounts of organic matter. The anomalous samples on the head of the southern canyons may be related to methanogenesis of recent drape or of older sidewall canyon infills.

INTRODUCTION

The Gulf of Lions (GoL) is a modern wave-dominated shelf where the tidal range is only a few cm, and waves have moderate energy (Rabineau et al., 1998). The margin is characterized by relatively low annual sediment inputs which are irregularly discharged over the years (Courp and Monaco, 1990); the Rhône river is the dominant (80%) source of sediment for the continental shelf.

A geostrophic current, known as the Liguro-Provençal current (LPC), flows south-westward along the continental slope. Its average speed near the seafloor on the outer shelf is 5 cm/s, reaching up to 30 cm/s (Millot, 1981; Millot and Crépon, 1981). The LPC current has an impact on sediment transport and deposition. A northern branch of this current is permanently flooding the shelf area, with a strong impact on the suspended particles from the Rhône plume and on the remobilized sediments (Aloïsi et al., 1979).

On the continental shelf, the associated currents to the LPC are often a few cm/s and almost negligible at the surface (Pinazo et al., 1996). Besides the western Mediterranean mesoscale circulation and the fresh water input of the Rhône river, the other main hydrodynamic features of this continental shelf are the strong northwestern (tramontane) and northern (mistral) winds, (Millot, 1999). The northwest sector winds, induced by a ridge of high pressure over the near Atlantic blow every other day and intensively throughout the year, encouraging the formation of coastal upwellings along the north coast (Estournel et al., 1997).

Fresh water inputs in the GoL vary throughout the year, with peaks in rainy seasons, generally spring and fall (Moutin et al., 1998), but the main input is the Rhône river plume (Petrenko et al., 2005), that sometimes extends all the way to the Spanish coast (Castellon et al., 1985). In the last (2003) flood event, the peak discharge of the Rhône was 13000 m^3/s (Kettner et al., 2004).

The annual budgets of primary production and new production for the GoL shelf are estimated at 71±7 and 37± 4 g C m-2 (Raimbault and Durrieu de Madron, 2003). The mean secondary production for the entire GoL is estimated at 54 mgC m-2 d-1 in spring and 19 mgC m-2 d-1 in winter, corresponding to 11-12% of the primary production (Gaudy et al., 2003). The GoL is characterized by phosphorus deficiency, which limits nitrate utilization by phytoplankton and is the main factor controlling primary productivity (Diaz et al., 2001).
During winter 2003-04, within the framework of the EuroSTRATAFORM project, seven submarine canyon heads along the GoL were monitored with instrumented moorings deployed at 300m water depth (Palanques et al., submitted). Results obtained during these deployments demonstrated that the Gulf of Lions submarine canyons are active conduits of sediment during present conditions, and that the major mechanisms contributing to sediment transport are eastern storms and shelf water cascading.

Shallow gas and indirect evidence

In the northern GoL indirect evidence for potential gas has been reported as ‘Tables’ facies, in particular all the prodelta areas up to 60 m depth (Aloïsi, 1986). Different types of acoustic masking in high-resolution seismic records are common features of the Rhône river. In the inner shelf, the prodeltaic sediments (0-30 m water depth) are essentially thin-layered silty muds (Chassefiere, 1990). Near the shoreline the prodeltas are frequently formed of ‘bubble-muds’ rich in methane, which escapes instantly upon physical disturbance, associated with muds enriched in plant debris and peats (Aloïsi

and Monaco, 1980). In the southern Cap de Creus canyon, a preliminary study shows almost no gas in the upper sedimentary record (García-García et al., in press).

The present paper presents two new headspace gas datasets taken along the western coast and also data from previously sampled sites off the Rhône river and Cap de Creus areas. The occurrence of the shallow gas (and organic carbon) is discussed, and integrated with previous data to better understand the occurrences of shallow gas in the gulf.

METHODOLOGY

EuroSTRATAFORM scientists examining the Gulf of Lions took advantage of a significant amount of previous work that had been conducted in the area, including the acquisition of high resolution seismic data (Aloïsi, 1986; Baztan et al., 2005; Rabineau et al., 2005). Sub-bottom data in the area had identified regions of anomalous to occluded sub-surface reflectivity, which had been interpreted as being due to the presence of shallow gas (Aloïsi, 1986). This study uses both the overall nature of anomalous sub-bottom character and its extent, and the nature of the margins (both vertically and horizontally) to infer an association with shallow gas. Our goals were to ground truth the interpretation of shallow gas origin from the anomalous sub-bottom character, and to understand the origin of this spatially restricted distribution of shallow gas.

We evaluated cores from the Gulf of Lions by sub-sampling the basal portion of kasten cores and box cores (see **figure 1**). Cores sub-sampled for shallow gas were acquired with the following research vessels: R/V Antedon II, R/V Tethys II, R/V Oceanus and the R/V Endeavor between February 2004 and May 2005. They were acquired along the western coast, focusing on the two edges of the GoL system, the Rhône prodelta and the southernmost canyons.

Station locations are designated by a letter indicating the coring transect (with letters ascending from north to south; each transect is oriented approximately perpendicular to isobaths), and a number indicating approximate water depth (e.g.: core F16 was acquired on the “F” transect in approximately 16m of water). Cores were acquired in water depths of 10 to 25m; no salinity measurements were taken at these sites during coring operations, or on the cores themselves. Although salinity affects gas accumulation, with lower salinity favoring gas higher up in the sediment column, we have no reason to believe that the samples in 10 to 25m of water come from varying salinity conditions. Instead, we believe samples in these water depths were thoroughly mixed with seawater prior to their deposition.

Cores were sampled for headspace gas in the following manner:

A 5-cm-long section near the base of the core was removed and placed into a metal can equipped with a septum and weighed. Next, the sample can was filled with water to the rim and 100 mL of water was removed. About 2 to 3 grams of sodium chloride salt was

added as a bactericide. The sample and water were sealed in the can leaving a 100mL headspace. The sealed can was then inverted and frozen. Frozen samples were transported to the organic geochemistry laboratory at the U.S.G.S. in Menlo Park, California where they were placed in a freezer. Samples were stored until they were thawed, processed and analyzed. Headspace analyses can provide an assessment of the constituents in a gas (C1, C2+, etc.), as well as a relative determination of gas concentrations. In this study, headspace analyses were conducted on a single sample from a core (typically the deepest undisturbed region) so that the rest of the core could be used by colleagues studying sediment accumulation rates, preservation of primary structures, etc. Although this sample may not be representative of the entire core, our experience has shown that the deepest sample, which has the highest probability of being below the methane oxidation – sulfate reduction horizon, typically has the highest gas concentrations.

Because headspace analyses measure gas concentrations on cores that are not pressurized (and thus can de-gas on their way to the surface), the measurements provide a minimum estimate of the amount of gas in a sample; absolute gas concentrations require pressurized sampling equipment to keep the gas from coming out of solution during ascent through the water column. For these samples, which originate in relatively shallow water, the headspace gas analyses would more closely relate to the actual concentration of gas than cores recovered from deeper water. Recovered samples with low concentrations of gas may be below saturation both at their original depth and at the sea surface. Headspace analyses of these samples may better reflect in situ gas concentrations. Note that the isotopic composition of the carbon in the methane would change very little even if there was degassing.

In the laboratory, the frozen samples in cans were allowed to thaw until they reached about 20℃, then placed into a high-speed shaker an d shaken for 5 minutes. The partitioned hydrocarbon gases in the headspace were analyzed for methane through hexane (C1-C6), CO_2, and H_2S by gas chromatography. Samples with more than 90 ppm methane are considered to be anomalous; background methane values in this and similar coastal environments are usually less than about 30 ppm.

Cores were sampled for organic matter (OM) analysis in the following manner:

Subcores, taken from the box-corer, were extruded onboard ship into 0-1 cm intervals. Only the uppermost (surficial) and the lowermost (bottom) sediment slices were used in this study. The lowermost slice is analogous to the sample collected for the gas analysis. Sediment samples for elemental and isotopic analyses were collected from sub-cores and refrigerated during transport back to the laboratory, then stored frozen until analysis. In the laboratory, the sample was dried at 55℃ and ground to pass through a 250 μm sieve prior to analysis.

Organic carbon (OC) and total nitrogen (TN) concentrations were obtained using a FISONS NA2000 Element Analyzer after removal of the carbonate fraction in silver capsules by dissolution in 1.5 N HCl. The average standard deviation of each

measurement, determined by replicate analysis of the standard, was ± 0.02 wt%. Stable isotopic analyses of organic carbon were carried out on the same samples using a FINNIGAN Delta Plus mass spectrometer, which was directly coupled to the FISONS NA2000 EA by means of a CONFLO interface for continuous flow measurements. The IAEA standard NBS19 was used as calibration material for carbon. Uncertainties were lower than ± 0.2 ‰, as determined from routine replicate measurements of the reference sample CH-7 (IAEA). Stable-isotope data are expressed in the conventional delta notation in which the $^{13}C/^{12}C$ isotopic ratios are reported relative to the international PDB standard.

RESULTS

Two new sets of data along the GoL margin were obtained between 2004 and 2005, on cruises, covering all the western GoL (**Figure 1**). Previous preliminary data had shown methane anomalies off the Rhône river and apparently no gas on the southern Cap de Creus canyon (García-García et al., in press, submitted). The link between both area was unknown until now though. These new data sets for the western GoL coast, along with pre-existing and new data from previous sites now enable a much fuller assessment of shallow gas occurrences in this region.

The headspace gas results are shown in **Table 1**. Out of 89 samples, 25 had anomalous gas content (more than 100 ppm of methane). Most of the samples were taken with a box core and only three of them were kasten cores (CC1670, LDRL296, LDRL472), none of which had anomalous gas. The headspace gas analyses show high anomalous methane peaks concentrated mainly off the Rhône river (see **figure 1**). Local anomalous methane contents also occur in the head of the southern canyons.

Most of the samples taken off the Rhône, had anomalous methane contents (see **figure 2**). Cores E33, F31, F32, G20, G31 have methane contents of 32680-95720 ppm (see **table 1**). All of them are located directly off the river, where the flood events are most influencial (García-García et al., in press).

With the idea of tracking the flood path, several cores were obtained along the western GoL (cores SO66 to TP28-see **figure 1**). Only core SF75 showed anomalous gas content (1840 ppm). Off the Rhône, multiple cores had anomalous gas content, but slightly further away, core SO66 showed no evidence of gas. For the first time, several samples for gas were taken on the head of the Lacaze-Duthiers canyon (**Figure 3**). Only core LSL93 had anomalous methane with a peak of 4982 ppm. The remaining cores in the area show no gas evidences. In the Cap de Creus area, core 3 had a gas content of 196 ppm.

Elemental and isotopic data

The biogeochemical analyses were focused in four areas of the Gulf of Lions: prodelta Rhône area, GoL shelf, Cap de Creus (CdC) shelf, CdC canyon. The uppermost and lowermost sediment was analyzed in each area except the GoL shelf, where the

lowermost slices were not studied. Kasten core analysis was carried out only for core K28 collected in front of the Rhône mouth. The elemental and isotopic data are presented on synthetic whisker plots for each area (**Figure 4**).

Depleted stable carbon isotope values were observed in the prodelta. The isotopic composition of the shelf and Cap de Creus canyon sediments was clearly "heavier". Each area showed a narrow range without exhibiting a clear variability among the uppermost slices and the lowermost ones.

The prodelta area showed the highest organic carbon content whereas the CdC canyon displayed the lowest contents of OC. In both areas the uppermost and the lowermost slices exhibited a different range. Notably, in the whisker plots the medians of the Rhône and the CdC shelf sediments are close, which does not show on the CdC canyon samples.

Concerning the nitrogen content, all whisker plots show a wide range and the relative medians are clearly different for each area. The highest total nitrogen contents were observed in the CdC shelf sediments and in the kasten core K28. The nitrogen measured in these sediments appears to be associated with OM (r-square > 0.8 and intercept close to 0 in all data sets; García-García et al., submitted), so we equate the organic nitrogen with the measured nitrogen values.

DISCUSSION

Stable isotopes and elemental data have been employed in biogeochemical investigations in coastal environments because they offer the potential to elucidate the roles of phytoplankton and vascular plants in the OC cycle (Hedges et al., 1997; Leithold and Hope, 1999; Gordon et al., 2001; Goñi et al., 1998). Vascular plants exhibit many bulk chemical and isotopic properties that distinguish them from marine phytoplankton (Hedges et al., 1997).

In terrestrial plants, carbon is taken directly from the atmosphere in the form of carbon dioxide with fractionation occurring during uptake of the dissolved gas into the cytoplasm via diffusion and then again during carboxylation (Park and Epstein 1961). Additionally, significant carbon fractionation can occur depending on the photosynthetic pathway (C3 versus C4) of carbon fixation (Fry and Sherr, 1984). C4 plants are most predominant in arid terrestrial environments (e. g. Teeri and Stowe, 1976). Significant variability is observed in the carbon isotopic composition of marine phytoplankton. Primary factors determining the fractionation of stable carbon isotopes in phytoplankton are carbon dioxide concentration, growth rate, cell size and cell shape (Fry and Sherr, 1984; Popp et al., 1998). As a result, the terrestrial plants (C3) exhibit δ^{13}OC values from -28 to 25 ‰ versus -22 to 19 ‰ for temperate marine plankton (Fry and Sherr, 1984). Another characteristic bulk property of most terrestrial plants is the predominance of nitrogen-free biomacromolecules; this raises the organic C/N ratio of characteristically carbon-rich plant tissues versus phytoplankton (C/N ≈ 7; Redfield et al., 1963).

In order to identify the origin of the sedimentary organic matter in the areas where the gas was collected, we plotted the OC isotopic composition versus the atomic ratio OC:TN of the Rhône Prodelta and CdC Canyon samples (**Figure 5**). The CdC samples are consistent with a marine origin whereas the Rhône prodelta samples are characterized by depleted values of δ^{13}OC and relatively high OC:TN ratios. Moreover, there is not a readily evident difference between the uppermost and lowermost layers in both data sets. Looking at the kasten core K28, terrestrial material clearly seems to influence this core which shows depleted δ^{13}OC; concerning the shelf samples, off the river mouth, the δ^{13}OC values become more positive (see **figure 4**) consistent with a predominantly marine origin. Plotting the superficial δ^{13}OC values of the uppermost layers on a contour map, a strong gradient is clearly visible when going offshore removed from any direct terrestrial input (**Figure 6a**). Finally, all prodelta samples (uppermost-lowermost layers and kasten core) exhibit a higher OC content whereas the rest of the samples display relatively low OC content, especially in the offshore stations (see **figures 4** and **figure 5**).

All these factors (depleted δ^{13}OC values, high OC:TN values and high OC contents) indicate a woody-debris contribution to the terrestrial material supplied by the river. Sand-sized plant fragments, rich in OC, hydraulically behave like very fine-sand (Leihtold and Hope, 1999), which might explain why this material is not found in the superficial sediment on the shelf and CdC Canyon where the OC content is isotopically "heavier" and the OM is relatively rich in nitrogen compared to carbon. Thill et al. (2001) estimated that almost all 50-200 μm particles are removed from surface water just off the mouth driven by settling and dilution processes and several studies have shown that the materials supplied by the Rhône river settle in a relatively small area close to the mouth (Guieu et al., 1993; Thomas, 1997). Only the soil, as terrestrial OM adsorbed to the finest material, can be subjected to resuspension events, which can efficiently transport these fine materials further offshore to an area below storm wave base (Roussiez et al., 2005). The selective transport and preservation in offshore regions of nonwoody vascular plants tissues has been observed in other shelves by many authors as elevated yields of cinnamyl versus vanillyl phenols (Hedges et al., 1997; Goñi et al.,1998) and this has been confirmed by lignin analyses on our samples (Tesi et al., 2006). For further details on the OM composition, Tesi et al. (in press) carried out CuO oxidations, elemental and stable carbon isotopic analyses performed on the same GoL stations.

We hypothesize that the woody debris is largely retained within the prodelta area, whereas the OC adsorbed on the finest material is initially deposited in the prodelta area and then, resuspended and transported westwards along the shelf following the general circulation (LPC). On its way, the OC looses its terrestrial signature by degradation and mixing with the "labile" marine OM which is easily remineralized on its way from the euphotic zone to the surficial sediment. As final result, the material that reaches the slope and the head of the CdC canyon is mainly marine and characterized by a relatively low OC content (see **figure 6b**). This is in agreement with Tesi et al. (in

press) which measured particularly low lignin contents in the distal shelf stations relative to the Rhône prodelta area.

Most of the samples taken off the Rhône, had anomalous methane contents (see **figure 2**). All of them are located directly off the river, where the flood events are most influencial. Previous headspace gas data off the Rhône showed a direct correlation between the flood events and the gas occurrences (García-García et al., in press). The new data acquired by revisiting some of those sites confirms the hypothesis that in the Rhône prodelta flood deposits deliver significant amounts of terrigenous organic matter that can be rapidly buried, effectively removing this organic matter from aerobic oxidation and biological uptake, and leading to the potential for methanogenesis with burial. In areas unaffected by this high flux of organic matter and rapid/thick flood deposition, or in between flood events, the conditions for methanogenesis and gas accumulation are not met. In these areas, the physical and biological reworking of the surficial sediment may effectively oxidize and mineralize organic matter and limit bacterial methanogenesis in the subsurface.

It seems the flood influence on the appearance of shallow gas is essentially limited to the river that the signal fades away quickly with distance. Off the Rhône, multiple cores have anomalous gas content, but slightly further away, core SO66 has no gas.

On the head of the Lacaze-Duthiers canyon (**Figure 3**) only core LSL93 shows anomalous methane. The rest of cores in the area showed no evidence of gas. The only anomalous sample could be explained by a local source. In the Cap de Creus area, core 3 shows an anomaly in its gas content. This core is located in the southern rim and the gas could be explained by material coming from the shelf. In the northern rim, three cores previously taken by García-García et al. (submitted) have high content of methane, but they can be explained by a local infill identified with high-resolution seismic records.

Compositional and isotopic analyses of the gas in the GoL area support a microbial origin although there are a few sites that show relatively heavy $\delta^{13}C$ values (-53 per mil) suggesting a mixed source for the gas.

From the Rhône, the path of the flood in the GoL can be traced along the coast to the south and when it reaches the CdC area, which is 200 km away, there is little organic matter available for methanogenesis. This could be the reason why there is so little shallow gas in the CdC. From a regional point of view, the occurrences of shallow gas seem to be related to the flood off the Rhône and to local sources at the head of the canyons. The rest of the GoL shows no evidence for accumulation of gassy sediments.

CONCLUSIONS

Anomalous methane contents up to 95720 ppm were found in samples taken from box cores off the Rhône prodelta. The Rhône flood deposits deliver significant amounts of terrigenous organic matter that can be rapidly buried, leading to the potential for

methanogenesis. Away from the flood-related sediments off the Rhône delta, the organic matter is being reworked and remineralized on its way along the western coast of the Gulf of Lions, with the result that the recent deposits in the southernmost canyons contain little reactive carbon. The few anomalous samples on the head of the southern canyons may be related to methanogenesis of recent drape or of older sidewall canyon infills.

The woody debris are retained within the prodelta area, whereas the OC adsorbed on the finest material is initially deposited in the prodelta area and then resuspended and transported westwards along the shelf following the general circulation. On its way the OC looses its terrestrial signature via degradation and mixing with the “labile” marine OM which is easily remineralized on its way from the euphotic zone to the surficial sediment. Consequently, the material that reaches the slope and the head of the canyons is mainly marine and characterized by a relatively low OC content.

ACKNOWLEDGEMENTS

We thank all of the scientific staff and crews from the R/V Oceanus, R/V Endeavor, R/V Antedon II and R/V Tethys II cruises as well as our EuroSTRATAFORM colleagues for their collaboration and assistance. We thank IFREMER for sharing the regional bathymetric dataset. The research herein was funded by the U.S. Navy through the Office of Naval Research EuroSTRATAFORM project (contract number N00014-03-1-142, Orange) and also funded by the contract number N00014-98-1-0073. We thank the University of Victoria (M. Whiticar) for isotopic analyses of headspace gases. This is ISMAR-Bologna contribution number 1529. Constructive reviews by Dr. Upstill-Goddard and an anonymous reviewer have improved the manuscript. We also thank editors Dr García-Gil and Dr. Judd for their help along the revision process.

REFERENCES

Aloïsi JC, Millot C, Monaco A, Pauc H (1979) Dynamique des suspensions et mécanismes sédimentologiques sur le plateau continental du Golfe du Lion. Comptes Rendus de l’Académie des Sciences de Paris, 289 D: 879-882

Aloïsi JC, Monaco A (1980) Etude des structures sédimentaires dans les milieux deltaïques (Rhône). Apport à la connaissance des conditions de sédimentation et de diagenèse. Comptes Rendís de l’Académie des Sciences de Paris, 290D: 159-162

Aloïsi JC (1986) Sur un Modèle de Sédimentation Deltaïque. Contribution à la connaissance des marges passives. Unpublished thesis. Université de Perpignan, France, 162 pp

Baztan J, Berné S, Olivet J-L, Rabineau M, Aslanian D, Gaudin M, Rehault J-P, Canals M (2005) Axial incision: The key to understand submarine canyon evolution (in the western Gulf of Lion). Mar Petrol Geol 22(6-7): 805-826

Castellon A, Salat J, Maso M (1985) Some observations on Rhone fresh water plume in the Catalan coast. In: CIES (Ed.), Rapp Comm Int Mer Medit Monaco, pp 119-121

Chassefiere B (1990) Mass-physical properties of surficial sediments on the Rhône continental margin: implications for the nepheloid benthic layer. Cont Shelf Res 10(9-10): 857-867

Courp T, Monaco A (1990) Sediment dispersal and accumulation on the continental margin of the Gulf of Lions: sedimentary budget. Cont Shelf Res 10: 1063-1087

Diaz F, Raimbault P, Boudjellal B, Garcia N, Moutin T (2001) Early phosphorus limitation during spring in the Gulf of Lions. Mar Ecol Progr Series 211: 51-62

Estournel C, Kondrachoff V, Marsaleix P, Vehil R (1997) The plume of the Rhône: numerical simulation and remote sensing. Cont Shelf Res 17(8): 899-924

Fry B, Sherr EB (1984) $\delta^{13}C$ measurements as indicators of carbon flow in marine and freshwater ecosystems. Mar Sci 27: 13–47

García-García A, Orange D, Lorenson T, Radakovitch O, Tesi T, Miserocchi S, Berné S, Friend PL, Nittrouer C, Normand A (in press) Shallow gas studies off the Rhône prodelta, Gulf of Lions. Mar Geol

García-García A, Orange D, Tesi T, Lorenson T, Sansoucy M, Herbert I, Miserocchi S, Dougherty J, Langone L (submitted) Cap de Creus: an active canyon with little shallow gas. Mar Geol

Gaudy R, Youssara F, Diaz F, Raimbault P (2003) Biomass, metabolism and nutrition of zooplankton in the Gulf of Lions (NW mediterranean). Oceanol Acta 26(4): 357-372

Goñi MA, Ruttenberg KC, Eglinton TI (1998) A reassessment of the sources and importance of land-derived organic matter in surface sediments from the Gulf of Mexico. Geoch et Cosmoch Acta 62: 3055–3075

Gordon ES, Goñi MA, Roberts QN, Kineke GC, Allison MA (2001) Organic matter distribution and accumulation on the inner Louisiana shelf west of the Atchafalaya River. Cont Shelf Res 21: 1691–1721

Guieu C, Zhang J, Thomas AJ, Martin JM, Brun-cottan JC (1993) Significance of atmospheric fallout on the upper layer water chemistry of the North Western Mediterranean. Jour Atm Chem 17: 45-60

Hedges JI, Keil RG, Benner R (1997) What happens to terrestrial organic matter in the ocean? Org Geochem 27: 195–212

Kettner AJ, Hutton EWH, Syvitski JPM (2004) Simulating the impact of the 2003 flood event of the Rhone river on the Gulf of Lions, France. EOS Trans AGU Fall Meeting 04 abstract

Leithold EL, Hope RS (1999) Deposition and modification of a flood layer on the northern California shelf: lessons from and about the fate of terrestrial particulate organic carbon. Mar Geol 154 : 183-195

Millot C (1981) La dynamique marine du lateau continental du golfe du Lion en étè. University of Paris 6, Unpub Doctor thesis

Millot C (1999) Circulation in the Western Mediterranean Sea. Jour Mar Sys 20: 423-442

Millot C, Crépon M (1981) Inertial oscillations on the continental shelf of the Gulf of Lions. Observations and theory. Jour Phys Oceanogr 11: 639-657

Moutin T, Raimbault P, Golterman HL, Coaste B (1998) The input of nutrients by the Rhône river into the Mediterranean Sea: recent observations and comparison with earlier data. Hydrobiologia 373-374 : 237-246

Palanques A, Durrieu de Madron X, Puig P, Fabres J, Guillén J, Calafat A, Canals M, Bonnin J (submitted) Suspended sediment fluxes and transport processes in the Gulf of Lions submarine canyons. The role of storms and dense water cascading. Mar Geol

Park R, Epstein S (1961) Metabolic fractionation of 13C and 12C in plants. Plant Physiol 36:133–138

Petrenko A, Leredde Y, Marsaleix P (2005) Circulation in a stratified and wind-forced Gulf of Lions, NW Mediterranean Sea: in situ and modeling data. Cont Shelf Res 25: 7-27

Pinazo C, Marsaleix P, Millet B, Estournel C, Véhil R (1996) Coupled modelling of physical and biological processes in the Gulf of Lions (northwestern Mediterranean): spatial and temporal variability. Jour Phys Oceanogr 23: 164-171

Popp BN, Laws EA, Bidigare RR, Dore JE, Hanson KL, Wakheman SG (1998) Effect of phytoplankton cell geometry on carbon isotopic fractionation. Geochim Cosmochim Acta 62: 69–77

Rabineau M, Berné S, Aslanian D, Olivet J-L, Joseph P, Guillocheau F, Bourillet J-F, Ledrezen E, Granjeon D (2005) Sedimentary sequences in the Gulf of Lion: A record of 100,000 years of climatic cycles. Mar Petrol Geol 22(6-7): 775-804

Rabineau M, Berné S, Ledrezen É, Lericolais G, Marsset T, Rotunno M (1998) 3D architecture of lowstand and transgressive Quaternary sand bodies on the outer shelf of the Gulf of Lion, France. Mar Petrol Geol 15: 439-452

Raimbault P, Durrieu de Madron X (2003) Research activities in the Gulf of Lion (NW mediterranean) within the 1997-2001 PNEC Project. Oceanol Acta 26(4): 291-298

Redfield AC, Ketchum BH, Richards FA (1963) The influence of organisms on the composition of seawater. In The Sea, Vol. 2 (ed. M. N. Hill), John Wiley, New York, pp 26–77

Roussiez V, Aloisi JC, Monaco A, Ludwig W (2005) Early muddy deposits along the Gulf of Lions shoreline: A key for a better understanding of land-to-sea transfer of sediments and associated pollutant fluxes. Mar Geol 222–223: 345– 358

Teeri JA, Stowe LG (1976) Climatic patterns and the distribution of C4 grasses in North America. Oecologia 23: 1–12

Tesi T, Miserocchi S, Goñi MA, Langone L (in press) Source, transport and fate of terrestrial organic carbon on the western Mediterranean Sea, Gulf of Lions, France. Mar Chem

Tesi T, Miserocchi S, Goñi MA, Langone L (2006) Comparative organic geochemistries in surficial sediments from the Rhône (France) and Po (Italy) prodelta area. Ocean Science Meeting, Honolulu (Hi) 20-24 February, OS16A-34

Thill A, Moustier S, Garnier JM, Estournel C, Naudin JJ, Bottero JY (2001) Evolution of particle size and concentration in the Rhône river mixingzone:influence of salt flocculation, Cont Shelf Res 21: 2127–2140

Thomas AJ (1997) Input of artificial radionuclides to the Gulf of Lions and tracing the Rhône influence in marine surface sediments. Deep Sea Res II 44: 577-595

Figures Captions

Figure 1. Location of cores in the Gulf of Lions during 2004-2005 cruises. Regional bathymetric map by IFREMER.2. Anomalous samples with high methane composition (>100ppm) shown as red stars (see table 1 for methane values). Insets show location of figures 3 and 4 of the paper.

Figure 2. Samples taken for headspace gas analyses off the Rhône river. Anomalous samples with high methane composition (>100ppm) shown as red stars (see table 1 for methane values).

Figure 3. Samples taken for headspace gas analyses on the two southernmost canyons, Lacaze-Duthiers and Cap de Creus. Anomalous samples with high methane composition (>100ppm) shown as red stars (see table 1 for methane values).

Figure 4. Elemental and isotopic composition (%OC, %TN, δ^{13}OC ‰) of organic matter in four areas of Gulf of Lions (GoL): Prodelta Rhône area, GoL Shelf, CdC Shelf, CdC Canyon. The 'uppermost' and 'lowermost' sediment slices are subcores taken from box-core. The lowermost slice was collocated with the sample collected for gas analysis.

Figure 5. Atomic OC:TN ratio versus stable carbon isotopic composition (δ^{13}OC ‰) of organic matter in bulk sediment collected in the Rhône prodelta area and Cap de Creus Canyon. Enclosed symbols represent the uppermost layers whereas open symbols represent the lowermost ones.

Figure 6a. Stable carbon isotopic distribution (δ^{13}OC ‰) of organic matter in surface sediment collected in the Rhône prodelta area and in shelf area; Figure 6b. Organic carbon distribution (OC) of organic matter in surface sediment collected in the Rhône prodelta area and in shelf area.

Table Caption

Table 1. Headspace gas analyses of the Gulf of Lions dataset. Anomalous methane contents are highlighted in bold.

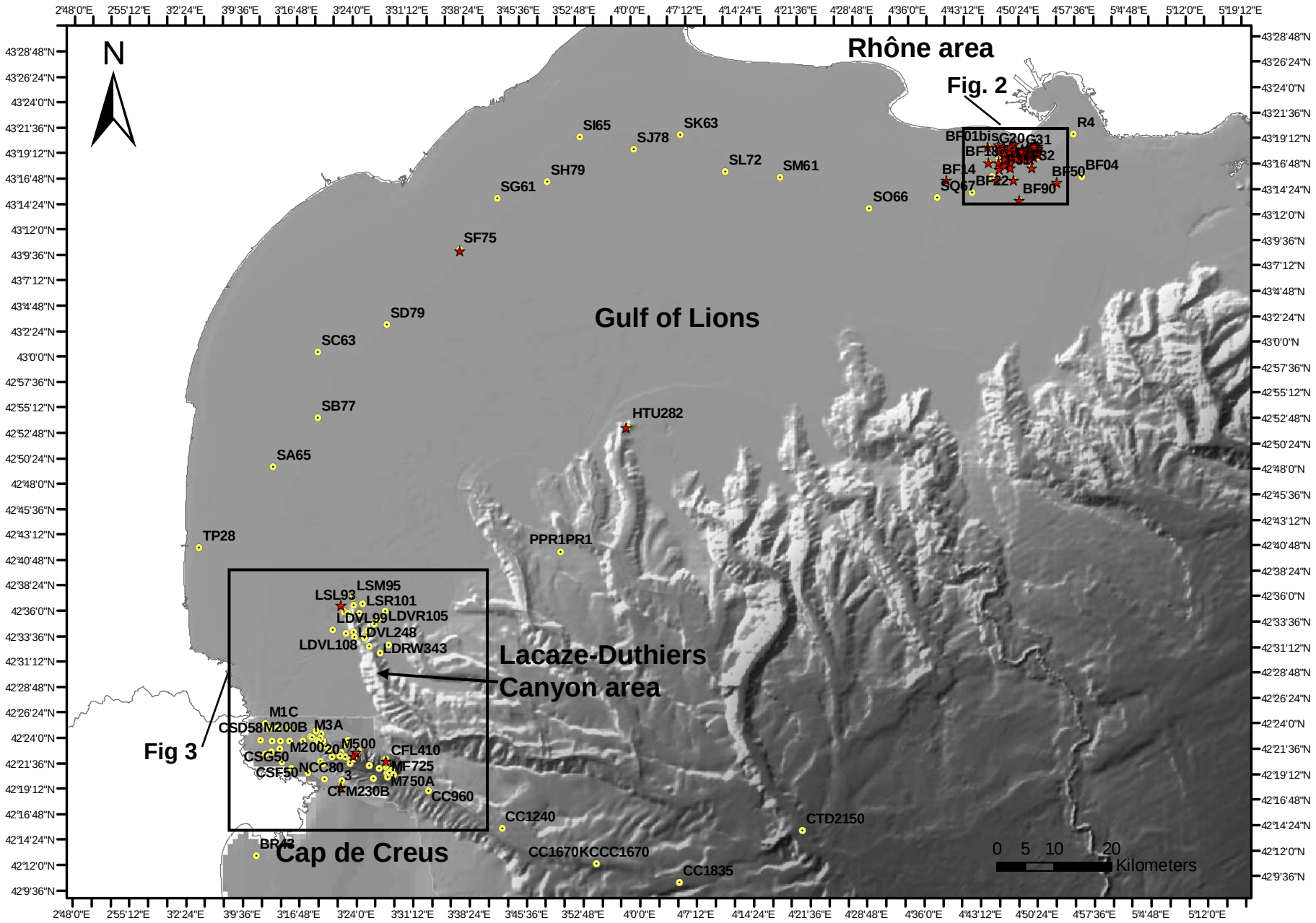
N
Rhône area
Fig. 2
Gulf of Lions
Lacaze-Duthiers
Canyon area
Fig 3
Cap de Creus
SI65
SK63
SJ78
SL72
SM61
SH79
SG61
SF75
SD79
SC63
SB77
SA65
TP28
HTU282
PPR1PR1
SO66
SQ67
R4
BF04
BF50
BF90
BF22
BF14
LSM95
LSL93
LSR101
LDVL99
LDVR105
LDVL248
LDVL108
LDRW343
M1C
CSD58
M200B
M3A
M500
CFL410
CSG50
M200
MF725
CSF50
NCC80
M750A
CFM230B
CC960
CC1240
CTD2150
BR43
CC1670K
CCC1670
CC1835
0 5 10 20
Kilometers

Fig 1.

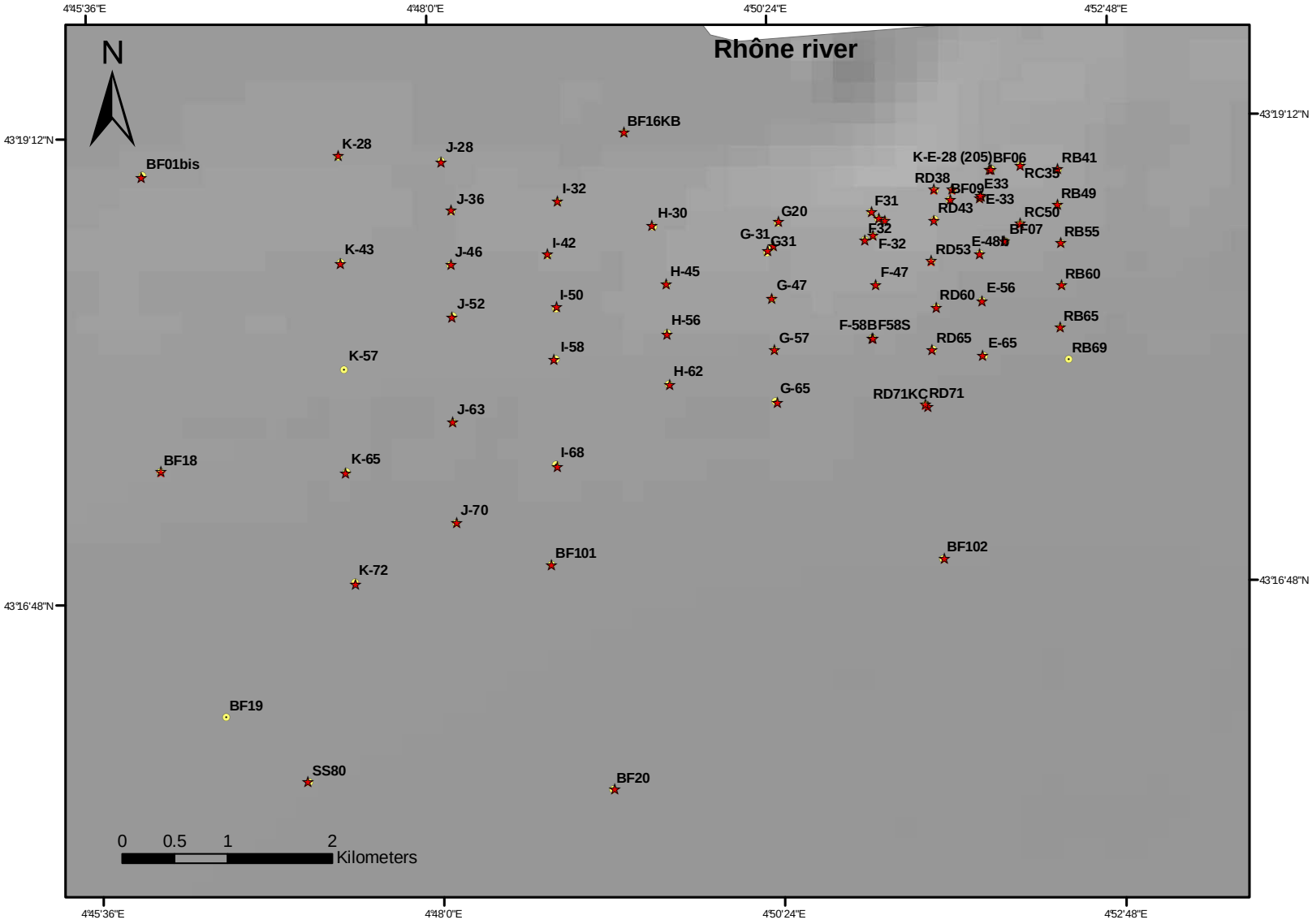
4°45'36"E
4°48'0"E
4°50'24"E
4°52'48"E
43°19'12"N
43°16'48"N
N
Rhône river
BF16KB
K-28
J-28
BF01bis
J-36
I-32
H-30
G20
F31
K-E-28 (205)
BF06
RB41
RD38
BF09
E33
RC35
RB49
RD43
E-33
RC50
F32
BF07
RB55
G-31
G31
F-32
E-48
K-43
J-46
I-42
RD53
H-45
F-47
RB60
G-47
E-56
I-50
J-52
RD60
H-56
F-58
BF58S
RB65
G-57
RD65
E-65
RB69
K-57
I-58
H-62
G-65
RD71KC
RD71
J-63
BF18
K-65
I-68
J-70
BF101
BF102
K-72
BF19
SS80
BF20
0
0.5
1
2
Kilometers

Fig 2.

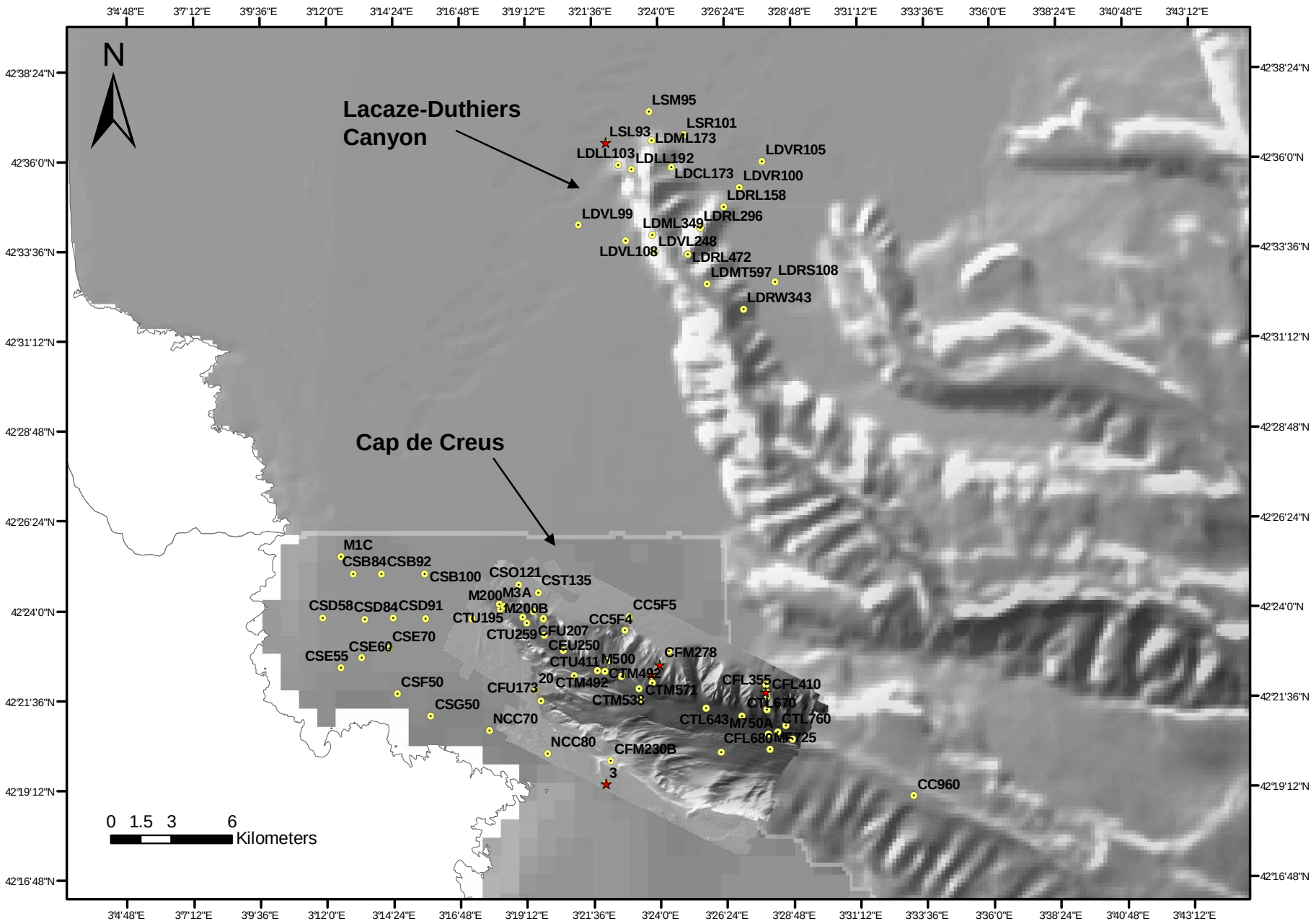
N
Lacaze-Duthiers Canyon
Cap de Creus
LSM95
LSR101
LSL93
LDML173
LDLL103
LDLL192
LDVR105
LDCL173
LDVR100
LDRL158
LDVL99
LDML349
LDRL296
LDVL248
LDVL108
LDRL472
LDMT597
LDRS108
LDRW343
M1C
CSB84
CSB92
CSB100
CSO121
CST135
M200
M3A
M200B
CSD58
CSD84
CSD91
CTU195
CC5F5
CC5F4
CTU259
CFU207
CSE70
CEU250
CSE60
CSE55
CFM278
CTU411
M500
CTM492
CSF50
CFU173
20
CTM492
CFL355
CFL410
CTM571
CTM538
CSG50
CTL643
M750A
CTL760
NCC70
CFL680
M725
NCC80
CFM230B
3
CC960
0 1.5 3 6
Kilometers
3°4'48"E
3°7'12"E
3°9'36"E
3°12'0"E
3°14'24"E
3°16'48"E
3°19'12"E
3°21'36"E
3°24'0"E
3°26'24"E
3°28'48"E
3°31'12"E
3°33'36"E
3°36'0"E
3°38'24"E
3°40'48"E
3°43'12"E
42°38'24"N
42°36'0"N
42°33'36"N
42°31'12"N
42°28'48"N
42°26'24"N
42°24'0"N
42°21'36"N
42°19'12"N
42°16'48"N

Fig 3.

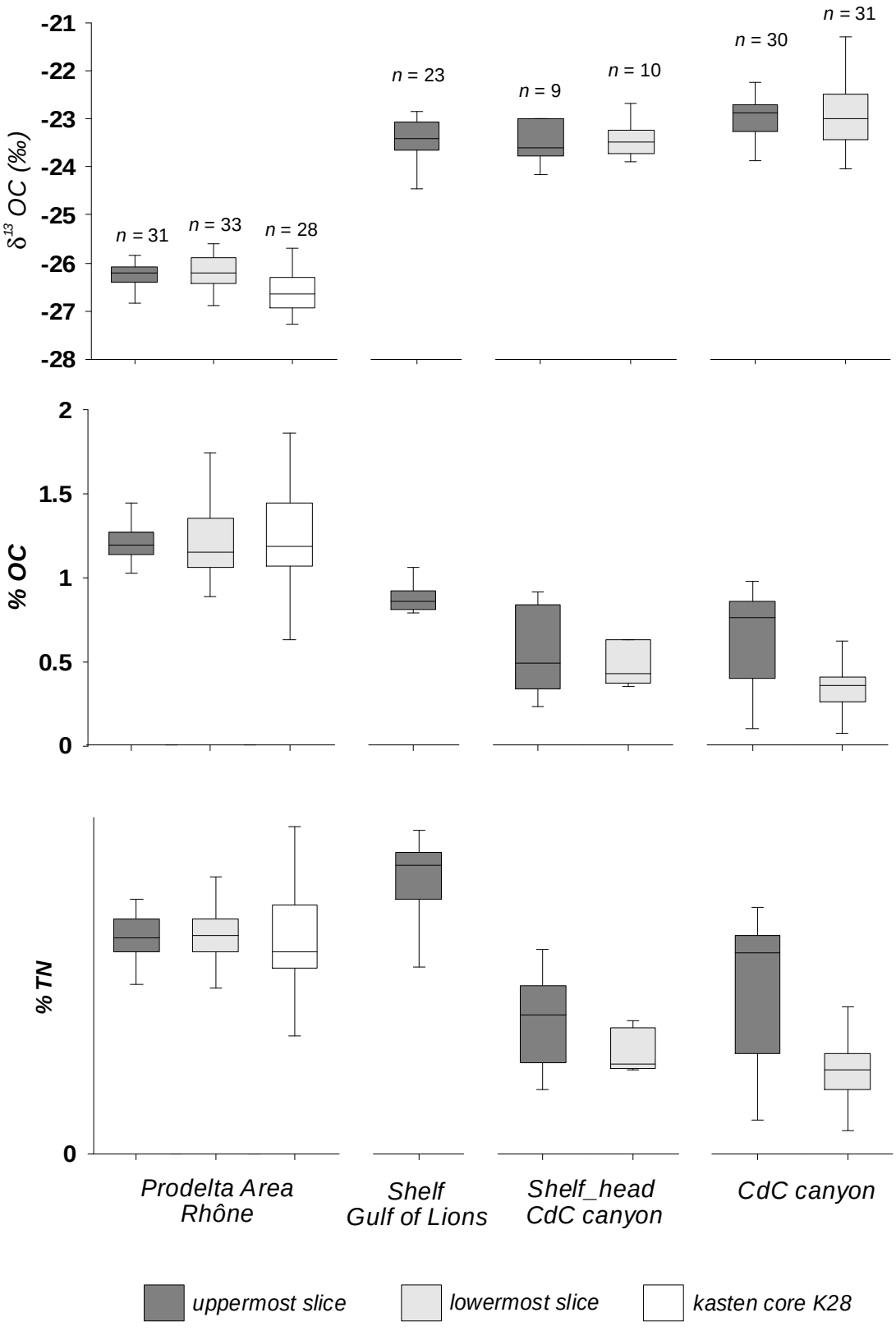
-21
-22
-23
-24
-25
-26
-27
-28
δ13 OC (‰)
n = 31
n = 33
n = 28
n = 23
n = 9
n = 10
n = 30
n = 31
2
1.5
1
0.5
0
% OC
0
% TN
Prodelta Area
Rhône
Shelf
Gulf of Lions
Shelf_head
CdC canyon
CdC canyon
uppermost slice
lowermost slice
kasten core K28

Figure 4.

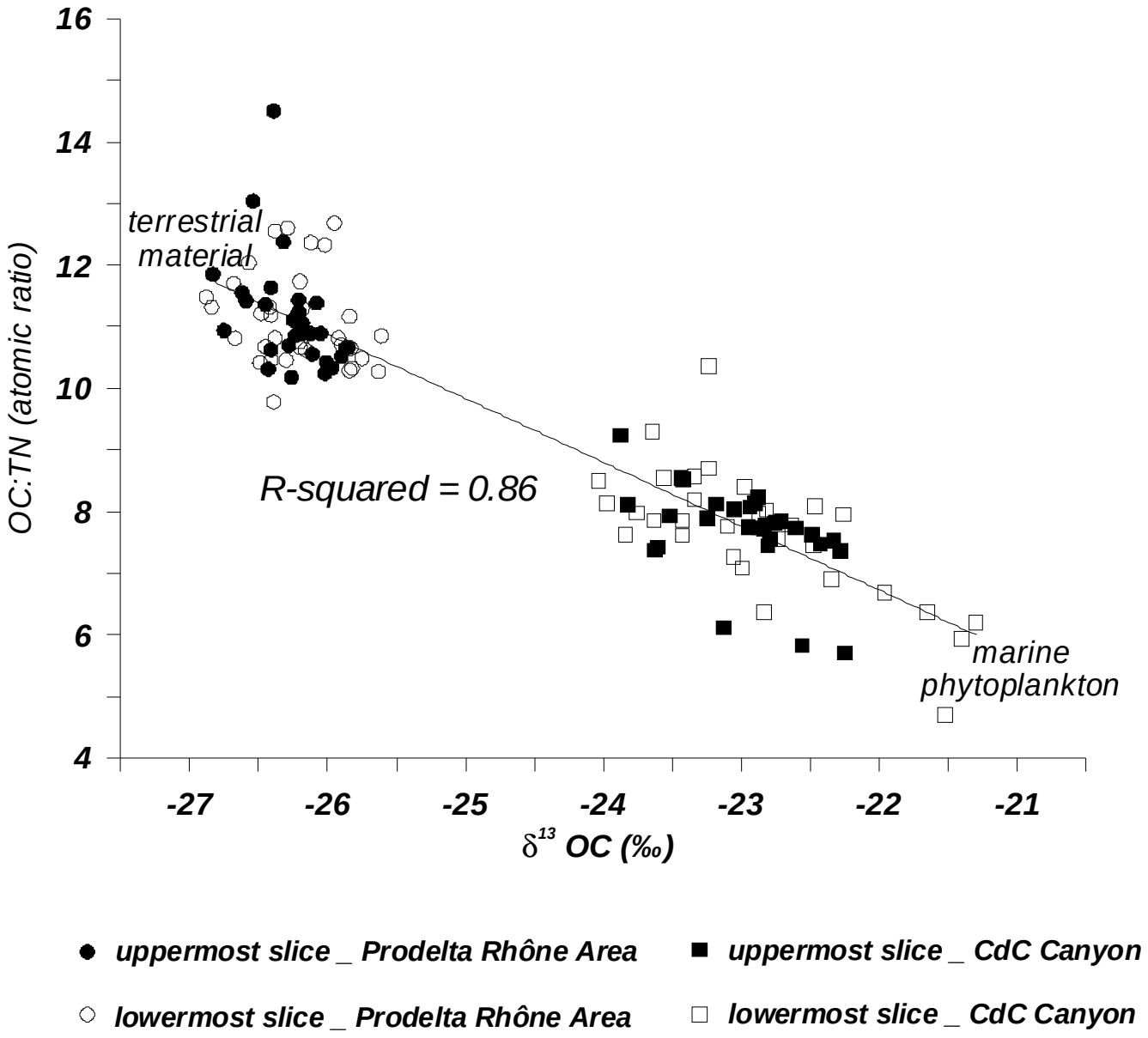
16
14
12
10
8
6
4
OC:TN (atomic ratio)
terrestrial material
R-squared = 0.86
marine phytoplankton
-27
-26
-25
-24
-23
-22
-21
δ13 OC (‰)
uppermost slice _ Prodelta Rhône Area
uppermost slice _ CdC Canyon
lowermost slice _ Prodelta Rhône Area
lowermost slice _ CdC Canyon

Figure 5.

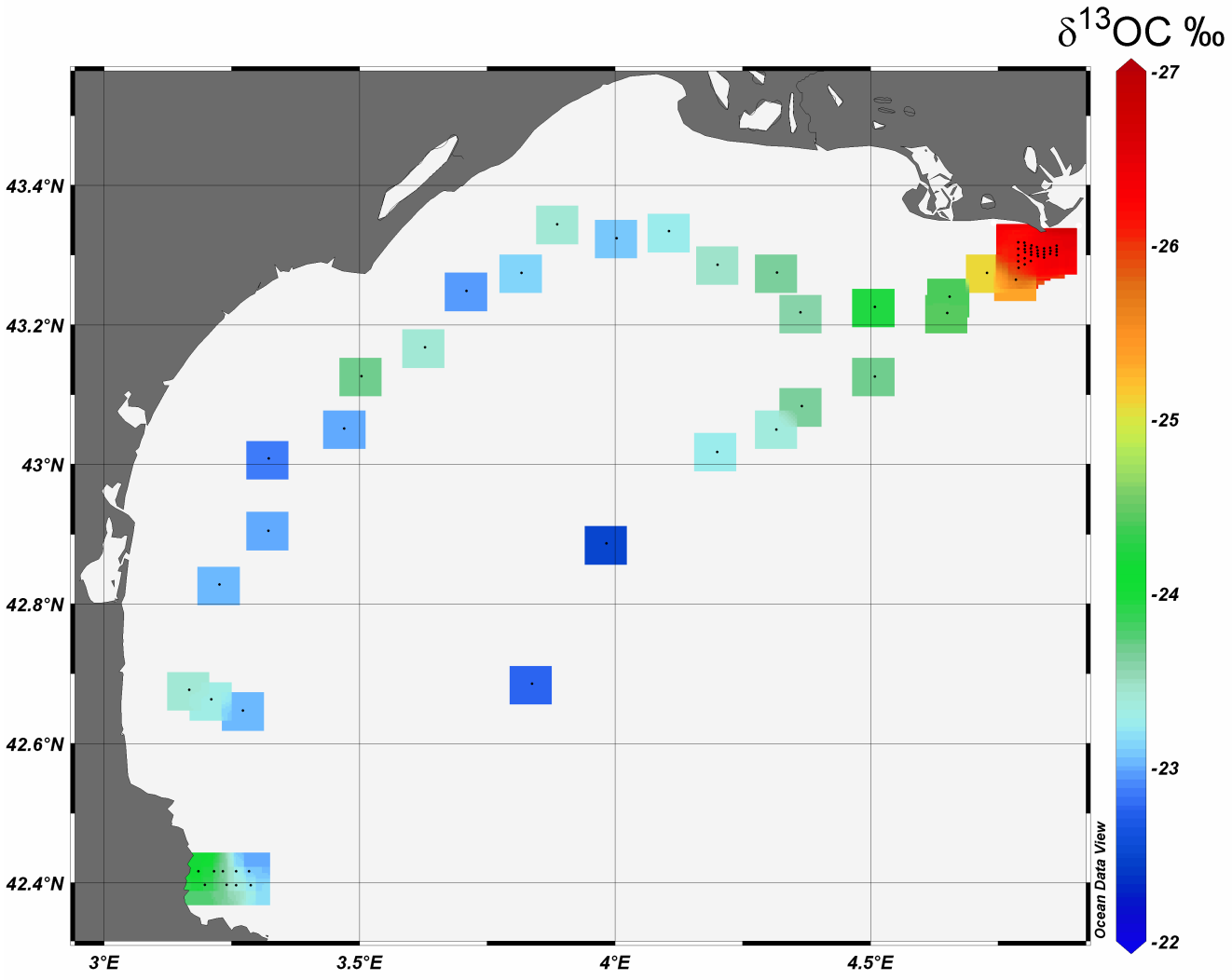
δ13OC ‰
-27
-26
-25
-24
-23
-22
43.4°N
43.2°N
43°N
42.8°N
42.6°N
42.4°N
3°E
3.5°E
4°E
4.5°E
Ocean Data View

Figure 6a.

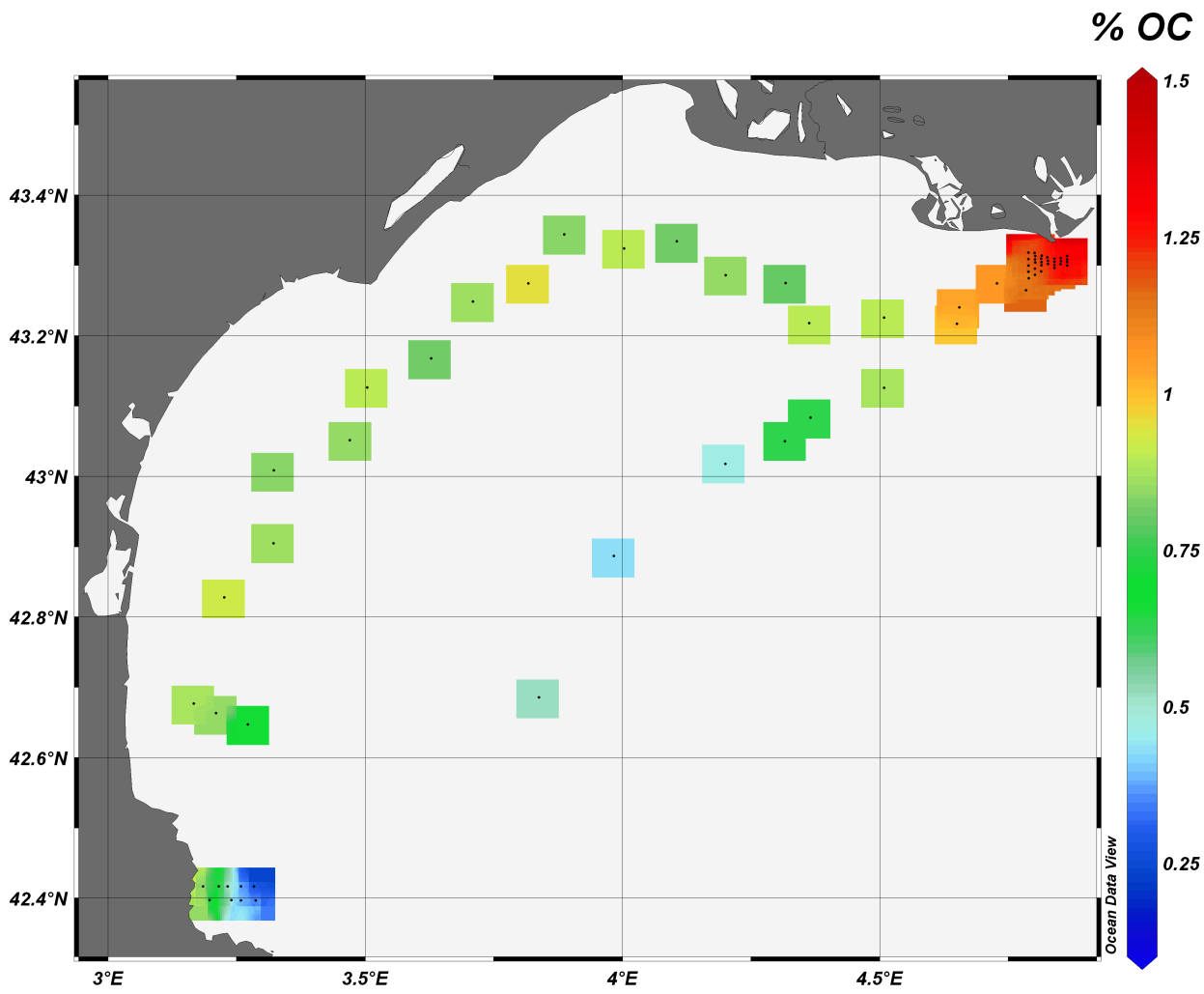
% OC
1.5
1.25
1
0.75
0.5
0.25
43.4°N
43.2°N
43°N
42.8°N
42.6°N
42.4°N
3°E
3.5°E
4°E
4.5°E
Ocean Data View

Figure 6b.

SITE	LONG	LAT	C1	C2	C3	CO2	C1	C2	C3	CO2
			(ppm)				(µL/L)			
3	3.3669	42.3230	**196.00**	0.90	0.15	2000	193.04	0.89	0.14	1900
20	3.3245	42.3647	9.41	0.34	0.10	8000	11.04	0.39	0.12	9500
BR43	3.1877	42.2160	25.61	0.97	0.13	9000	36.59	1.39	0.19	13300
CC1240	3.7079	42.2570	3.19	0.51	0.19	10000	3.77	0.60	0.23	12100
CC1670	3.9065	42.1991	7.68	0.77	0.24	9000	5.86	0.59	0.18	6900
CC1670KC	3.9066	42.1992	11.02	0.46	0.08	8000	8.45	0.35	0.06	6300
CC1835	4.0827	42.1689	76.16	0.82	0.25	9000	54.40	0.59	0.18	6800
CC5F4	3.3785	42.3913	16.62	0.64	0.17	8000	16.01	0.61	0.16	7700
CC5F5	3.3813	42.3974	5.89	0.48	0.19	7000	7.82	0.63	0.25	9900
CC960	3.5517	42.3168	5.52	0.18	0.23	7000	5.06	0.17	0.21	6600
CEU250	3.3303	42.3890	4.67	0.77	0.10	9000	4.52	0.75	0.10	9000
CFM230B	3.3697	42.3333	5.48	0.99	0.12	9000	3.86	0.70	0.09	6600
CFM300	3.3687	42.3779	4.35	0.60	0.06	8000	6.17	0.85	0.09	11500
CFU207	3.3298	42.3962	4.06	0.62	0.11	9000	5.24	0.80	0.14	11600
CSE55	3.2079	42.3750	19.83	0.74	0.14	10000	19.55	0.73	0.14	10000
CSE60	3.2206	42.3796	21.07	0.44	0.08	11000	17.42	0.36	0.06	8800
CSE70	3.2369	42.3839	4.92	0.85	0.17	8000	5.24	0.90	0.18	8900
CSF50	3.2419	42.3635	13.63	0.58	0.17	9000	13.70	0.58	0.17	9000
CSG50	3.2619	42.3536	6.13	0.60	0.12	8600	5.96	0.58	0.11	8400
CST135	3.3266	42.4084	5.17	0.56	0.05	8800	4.10	0.44	0.04	6900
CTD2150	4.3438	42.2476	5.21	0.57	0.14	7800	3.23	0.35	0.09	4800
CTM492	3.3667	42.3731	6.93	0.75	0.15	7800	6.39	0.69	0.14	7200
E33	4.8647	43.3136	**47000.00**	0.00	0.41	9900	56000.00	0.00	0.49	11900
F31	4.8519	43.3125	**95700.00**	0.00	1.16	13300	75000.00	0.00	0.91	10400
F32	4.8510	43.3100	**33000.00**	0.00	0.96	17600	25000.00	0.00	0.74	13500
G20	4.8408	43.3116	**48000.00**	0.00	0.45	10500	90000.00	0.00	0.84	19600
G31	4.8395	43.3090	**93000.00**	0.00	1.29	13300	90000.00	0.00	1.26	13000
LDCL173	3.4077	42.5974	13.50	0.53	0.11	8500	10.58	0.42	0.09	6600
LDLL103	3.3761	42.5985	3.66	0.81	0.12	8800	2.32	0.51	0.07	5600
LDLL192	3.3840	42.5964	5.10	0.60	0.18	10000	4.07	0.48	0.14	8000
LDML173	3.3960	42.6095	6.27	0.57	0.18	7700	5.56	0.51	0.16	6800
LDML349	3.3960	42.5671	12.22	0.76	0.19	7900	13.37	0.83	0.21	8600
LDMT597	3.4290	42.5453	6.90	0.58	0.19	7900	7.88	0.67	0.22	9000
LDRL158	3.4392	42.5798	4.52	0.45	0.11	7800	3.42	0.34	0.08	5900
LDRL296KC	3.4250	42.5703	14.16	0.24	0.04	100	13.40	0.22	0.04	100
LDRL296	3.4251	42.5702	3.86	0.35	0.07	8000	3.88	0.35	0.07	8000
LDRL472	3.4179	42.5586	5.44	0.57	0.16	300	7.01	0.74	0.20	400
LDRL472KC	3.4179	42.5586	7.13	0.70	0.20	10500	6.01	0.59	0.17	8900
LDRS108	3.4698	42.5461	5.75	0.66	0.21	8100	5.80	0.66	0.22	8200
LDRW343	3.4511	42.5342	6.62	0.67	0.15	8600	5.96	0.60	0.14	7800
LDVL108	3.3800	42.5646	4.40	0.40	0.23	7700	3.90	0.35	0.20	6800
LDVL248	3.3977	42.5592	6.47	0.67	0.11	8200	7.59	0.78	0.13	9600
LDVL99	3.3516	42.5716	16.01	0.58	0.17	7900	9.13	0.33	0.09	4500
LDVR100	3.4489	42.5885	9.76	0.42	0.12	7600	7.70	0.33	0.10	6000
LDVR105	3.4627	42.6000	7.09	0.49	0.12	6000	5.08	0.35	0.08	4300
LSL93	3.3686	42.6085	**5000.00**	0.65	0.09	7400	4000.00	0.47	0.06	5400

Table 1.

SITE	LONG	LAT	C1	C2	C3	CO2	C1	C2	C3	CO2
			(ppm)				(µL/L)			
LSM95	3.3943	42.6224	24.02	0.63	0.22	1700	18.08	0.47	0.17	1300
LSR101	3.4154	42.6119	4.49	0.73	0.16	2900	3.20	0.52	0.12	2100
M1C	3.2079	42.4246	17.40	0.88	0.22	9000	14.79	0.75	0.19	7700
M200	3.3040	42.4019	7.88	0.54	0.06	7500	5.95	0.41	0.04	5700
M200B	3.3037	42.4009	20.95	0.84	0.12	8200	15.60	0.62	0.09	6100
M3A	3.3032	42.4033	5.96	0.60	0.08	8600	3.89	0.39	0.05	5600
M500	3.3619	42.3736	3.66	0.47	0.10	7500	4.57	0.59	0.12	9400
M750A	3.4644	42.3448	3.40	0.18	0.18	7200	3.82	0.21	0.20	8100
MF725	3.4657	42.3380	3.14	0.36	0.23	7800	3.81	0.43	0.27	9500
NCC70	3.2971	42.3473	4.61	4.38	0.17	8300	5.47	5.19	0.20	9900
NCC80	3.3317	42.3366	17.84	0.43	0.12	7300	19.41	0.47	0.13	8000
RB41	4.8739	43.3156	**1000.00**	0.51	0.35	6600	2000.00	0.77	0.52	10000
RB49	4.8737	43.3126	**48000.00**	0.00	0.47	10200	46000.00	0.00	0.44	1000
RB55	4.8740	43.3093	**2000.00**	0.96	0.39	12600	2000.00	1.00	0.40	13100
RB60	4.8740	43.3057	**2000.00**	0.82	0.75	11900	2000.00	0.89	0.81	12900
RB65	4.8737	43.3021	**283.00**	1.07	0.65	15500	224.09	0.85	0.51	12300
RB69	4.8746	43.2994	80.42	0.76	0.18	4300	61.41	0.58	0.13	3300
RC35	4.8695	43.3161	**9000.00**	0.06	1.14	5100	13000.00	0.08	1.57	7000
RC50	4.8693	43.3111	**285.00**	0.61	0.84	11300	241.28	0.52	0.71	9600
RD36	4.8613	43.3141	**67000.00**	0.00	1.16	15900	55000.00	0.00	0.95	13000
RD38	4.8593	43.3141	**87000.00**	0.00	0.88	13200	67000.00	0.00	0.68	10100
RD43	4.8592	43.3115	**88000.00**	0.00	1.23	18100	61000.00	0.00	0.84	12500
RD53	4.8588	43.3080	**51000.00**	0.00	0.64	13000	46000.00	0.00	0.58	11700
RD60	4.8592	43.3041	**675.00**	1.58	0.48	11900	647.13	1.52	0.46	11400
RD65	4.8587	43.3005	**270.00**	0.83	0.33	12400	311.93	0.96	0.38	14300
RD71	4.8577	43.2957	**171.00**	1.85	0.34	6200	101.87	1.11	0.20	3700
RD71KC	4.8578	43.2956	**306.00**	1.15	0.54	16200	343.66	1.29	0.60	18200
SA65	3.2256	42.8278	16.63	0.72	0.28	9900	12.21	0.53	0.20	7300
SB77	3.3218	42.9046	16.95	0.82	0.33	9700	12.58	0.61	0.24	7200
SC63	3.3224	43.0086	18.27	0.47	0.11	9400	18.62	0.48	0.12	9600
SD79	3.4700	43.0513	7.34	0.73	0.16	8200	7.45	0.74	0.16	8300
SF75	3.6284	43.1675	**2000.00**	0.62	0.31	1700	2000.00	0.61	0.30	1700
SG61	3.7093	43.2486	18.61	0.56	0.30	9100	15.38	0.46	0.25	7500
SH79	3.8168	43.2741	16.18	0.67	0.27	8900	16.02	0.66	0.27	8900
SI65	3.8870	43.3439	11.46	0.40	0.21	2800	9.29	0.33	0.17	2300
SJ78	4.0031	43.3238	8.77	0.58	0.14	8900	8.60	0.57	0.13	8800
SK63	4.1054	43.3442	7.39	0.57	0.12	7500	9.34	0.72	0.15	9500
SL72	4.2005	43.2858	7.79	0.41	0.10	400	9.14	0.48	0.11	500
SM61	4.3171	43.2749	5.89	0.49	0.10	7900	6.58	0.55	0.11	8800
SO66	4.5087	43.2254	27.72	0.48	0.08	10000	33.84	0.58	0.10	12200
SQ67	4.6550	43.2404	20.52	0.68	0.12	9900	20.42	0.68	0.12	9900
SS80	4.7845	43.2648	**2000.00**	0.78	0.09	1700	4000.00	1.48	0.16	3100
TP28	3.0674	42.7013	5.62	0.32	0.10	7700	4.32	0.25	0.07	5900

Table 1 (continuation).